Polymer Chemistry

Accepted Manuscript

ROYAL SOCIETY OF CHEMISTRY

www.rsc.org/polymers

Effect of Fluorine Substitution on the Photovoltaic Performance of Poly(thiophene-quinoxaline) Copolymers

Zi Qiao[1,2], Meng Wang[1,2], Mingzhi Zhao[1,2], ZhiGuo Zhang[3], Yongfang Li[3]*, Xiaoyu Li[1,2*], Haiqiao Wang[1,2*]

1. State Key Laboratory of Organic-Inorganic Composite, Beijing University of Chemical Technology, Beijing 100029, China

2. Key Laboratory of Carbon Fiber and Functional Polymers, Ministry of Education, Beijing University of Chemical Technology, Beijing 100029, China

3. Beijing National Laboratory for Molecular Sciences, Institute of Chemistry, Chinese Academy of Sciences, Beijing 100190, China

Abstract

In order to investigate the effects of fluorine atoms on the photovoltaic performance, three 2-D D-A conjugated copolymers, namely PT-QX (0F), PT-FQX (1F) and PT-DFQX (2F), were designed and synthesized using alkylthienyl substituted quinoxaline with different numbers of F substituents as acceptor unit and thiophene as donor unit. The physicochemical and photovoltaic properties were comparatively studied in details. The results demonstrate that the highest occupied molecular orbital (HOMO) energy levels are gradually lowered from -5.10 eV, to -5.18 eV and then to -5.33 eV for PT-QX (0F), PT-FQX (1F) and PT-DFQX (2F), respectively, while the lowest occupied molecular orbital (LUMO) energy levels nearly kept constant as the increase of F substituents. Introducing F on the polymer backbone widens the energy bandgap and makes the absorption peaks of the polymers blue-shifted. The highest

power conversion efficiencies of bulk heterojuncton polymer solar cells increased with the increase of F substituents from 2.82% for PT-QX (0F) to 4.14% for PT-FQX (1F) to 5.19% for PT-DFQX (2F) thanks to the enhanced V_{oc} and J_{sc}, The enhanced V_{oc} and J_{sc} can be mainly ascribed to the lower HOMO energy levels and moderate hole mobility of the fluorinated polymers, as well as better morphology and preferential orientation of face-on structure of the blend films of the fluorinated polymers donor with $PC_{71}BM$ acceptor.

1. Introduction

Over the past years polymer solar cells (PSCs) have attracted significant attention due to their predominant advantages of light-weight, low-cost, flexibility, and environmental friendly compared with the conventional inorganic solar cells.[1] Recently, the research on PSCs advances rapidly, which is mainly attributed to the development of photovoltaic materials and innovation of device fabrication technology. The power conversion efficiencies (PCEs) of bulk heterojuncton (BHJ) PSCs have reached over 10%,[2] which offers a promising future to their commercialization.

Donor−acceptor (D−A) type conjugated copolymers as electron-donating materials have become the most successful strategy for achieving high performance PSCs, because intramolecular charge transfer (ICT) from an electron-donating unit to an electron-accepting moiety allows for fine-tuning of band gaps, frontier molecular orbital energies, and light absorption strength.[3] Extensive research has provided some general guidelines for developing D-A conjugated copolymers.[4] Many literatures reported that introducing functional fluorine atoms into the polymers is an important and valid approach for improving the photovoltaic and physicochemical properties of D-A conjugated copolymers.[5]

Commonly, introduction of fluorine atoms into polymer chains is considered as an effective way to lower the energy levels of the polymers because of the strong electron-withdrawing nature of the fluorine atom.[6] As a result, fluorinated polymers

exhibit deeper HOMO energy levels, and thus afford higher open circuit voltage (V_{oc}) in BHJ PSCs. Meanwhile, some of the literatures reported that introduction of fluorine atoms enhanced inter/intramolecular interaction of polymers due to strongly induced dipole in C-F bond, which leads to higher charge carrier mobility and facilitate charge transfer.[7] Furthermore, it is also found that strong F···H/ F···S interactions and well-developed fibril structure in fluorine-containing polymers can contribute to appropriate morphology of the active layer and suppress charge recombination.[8]

So far, there are lots of literatures reporting the effect of F atom on photovoltaic performance of polymers. However, it is noteworthy that some literatures drew very different conclusions based on different systems. For example, some researchers found that F atoms can lower both HOMO and LUMO energy level,[9] but there was also literature reporting that the F atom can only lower HOMO energy level, and almost scarcely affect LUMO energy[10]; Yong Zhang *et al*. found that the F atoms cause the loss of hole-mobility of the photovoltaic polymers and result in decreased J_{sc} and FF of the PSCs [11]; In addition, the effect of the F atoms on absorption spectrum is also found to be different. Akila Iyer *et al*. observed that fluorination can effectively broaden the absorption spectra[12], but Bob Schroeder *et al*. reported that fluorination show negative effect on absorption[13]. Obviously, the effect of the F atoms on energy level, absorption spectrum and other photovoltaic performances is complicated, and depends on different polymer systems. Thus, it is of prime importance to fully understand the effects of the F atom on the physicochemical and photovoltaic properties in the design of new polymers for efficient PSCs.

In this contribution, we designed and synthesized three new D-A copolymers, PT-QX(0F), PT-FQX(1F) and PT-DFQX(2F), based on alkylthiophene substituted quinoxaline acceptor unit and thiophene donor unit, as shown in Scheme 1. For the convenience of study on the effects of the F atom, the three copolymers were built by non-fluorinated quinoxaline acceptor unit for PT-QX (0F), mono-fluorinated quinoxaline acceptor unit for PT-FQX (1F) and difluorinated quinoxaline acceptor unit for PT-DFQX (2F), respectively. The quinoxaline unit was selected as acceptor building block because it possesses strong electron affinity, and the facile synthesis

process and versatility make the quinoxaline unit become one of the most popular electron acceptor units copolymerized with various electron-donor (D) units.[14] In addition, in order to broaden the absorption and improve the solubility of the copolymers, two alkylthiophene π-conjugated side chains were introduced into the quinoxaline unit.[15] BHJ PSCs were fabricated based on the three copolymers as donor to investigate the effects of the F atoms. The highest PCE achieved for PT-QX(0F), PT-FQX(1F) and PT-DFQX(2F)–based PSCs are 2.82%, 4.14% and 5.19%, respectively, and it is found that J_{sc}, V_{oc} and FF of the corresponding PSCs enhanced with the increase of the fluorine atom substituents of the donor polymers. The results indicate that introducing F atoms into quinoxaline is a promising strategy to comprehensively improve the photovoltaic performance of the quinoxaline-based copolymer donor materials.

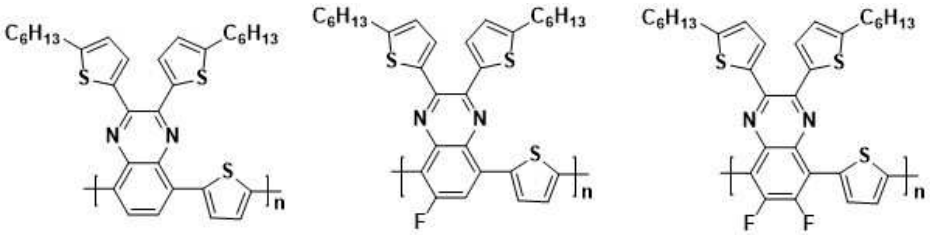

Scheme 1. The molecular structures of polymers PT-QX(0F), PT-FQX(1F) and PT-DFQX(2F).

2. RESULTS AND DISCUSSION

2.1 Synthesis and characterization

The synthesis routes of the copolymers are depicted in Scheme 2 and the detailed synthetic processes are described in experimental section. All the compounds **1-4** and **M1-3** were satisfactorily characterized by ^{1}H NMR, ^{13}C NMR and elemental analysis. PT-QX (0F), PT-FQX (1F) and PT-DFQX (2F) were prepared by Stille coupling polymerization reaction between the corresponding monomers catalyzed by $Pd_2(dba)_3$/P(*o*-tol)$_3$. The synthesized polymers were purified by continuous extractions with methanol, hexanes and chloroform, and the chloroform fractions were recovered.

All the polymers are highly soluble in common organic solvents such as chloroform, chlorobenzene and o-dichlorobenzene (DCB) at room temperature. Table 1 summarized the number-average molecular weight (M_n), weight-average molecular weight (M_w), the polydispersity index (PDI) (measured by GPC in Trichlorobenzene (TCB) at 150°C with polystyrene standards) and thermal properties of the copolymers. The M_n values of PT-QX (0F), PT-FQX (1F) and PT-DFQX (2F) are13.1, 14.3, and 16.6 kDa, respectively, with PDIs of 1.58, 1.73 and 1.73, respectively (Table 1). These indicate that the introduction of fluorine atoms have no significant influence on the molecular weight of the copolymers[16]. The thermal transition and stability of polymers were measured by TGA and DSC. DSC scans (Fig S1†) of the three polymers revealed that there were no evident phase transitions up to 250 °C. As shown in Fig S2† and Table 1, TGA thermograms showed that PT-QX (0F), PT-FQX (1F) and PT-DFQX (2F) are thermally stable with onset decomposition temperatures corresponding to 5% weight loss at 394, 381 and 348°C, respectively. The results indicate that all the polymers are stable enough for application in PSCs and can be potentially annealed at elevated temperatures.

Table 1. Molecular Weights and Thermal Properties of the Polymers

Polymer	M_n [a]	M_w [a]	PDI(M_w/M_n)[a]	T_d (°C)[b]
PT-QX (0F)	13.1K	20.7K	1.58	394
PT-FQX (1F)	14.3K	24.7K	1.73	381
PT-DFQX (2F)	16.6K	28.6K	1.73	348

[a]M_n, M_w and PDI of the polymers were estimated by GPC using polystyrene as standards in TCB. [b]The 5% weight-loss temperatures in nitrogen.

2.2 Optical properties

The normalized optical absorption spectra of these polymers in dilute chloroform and as thin films deposited on quartz glass are shown in Fig 1. Meanwhile the absorption peak wavelengths (λ_{max}), absorption edge wave lengths (λ_{onset}), and the optical band gap (E_g^{opt}) are summarized in Table 2. As shown in Fig 1, all these three polymers show similar absorption profile and have two characteristic absorption bands. The

higher energy band in the wavelength range of 300-500 nm arises from the localized π-π transition and intrinsic absorptions of alkylthiophene substituted quinoxaline unit[17], whereas a relatively broad and weak absorption in the wavelength range of 500-750 nm can be attributed to the intramolecular charge transfer (ICT) between the strong electron-accepting quinoxaline units and the electron-donating thiophene units. Compared with the absorption in solution, the lower energy band absorption strength of the polymer films improved significantly and the absorption peak appears evident red-shifts, as well as the shoulder peak around 450nm weakened or disappeared, indicating that aggregation of the polymer main chains and π-π intermolecular interactions existed in the solid film state. It should be noted that upon fluorination, PT-FQX (1F) and PT-DFQX (2F) exhibited vibronic features at low-energy absorption band in thin film. Whereas, this peak is completely absent in PT-QX (0F) suggesting that fluorination of quinoxaline moiety does not hinder backbone planarization and actually enhances intermolecular interaction. In addition, the introduction of fluorine atoms is advantageous to form aggregation of the conjugated backbones and π-π stacks that favor the charge transfer[18]. We speculate that the non-covalent interaction between fluorine atoms and components on adjacent aromatics are responsible for this phenomenon. It is also worth noting that both in solution and solid film state, the related absorption spectrum showed a slight blue-shift as the number of fluorine atom increased, which was also found by other groups. The electron-withdrawing nature of the fluorine atoms may lead to a permanent shift of π electrons and weaken the conjugation effect, which results in the blue-shifted UV-Vis absorption[19]. The E_g^{opt} of PT-QX (0F), PT-FQX (1F) and PT-DFQX (2F) were calculated from the λ_{onset} of the polymer film are 1.61 eV, 1.68 eV and 1.77 eV respectively, this indicates that introducing F on the polymer backbone broadened the optical bandgap of the polymers.

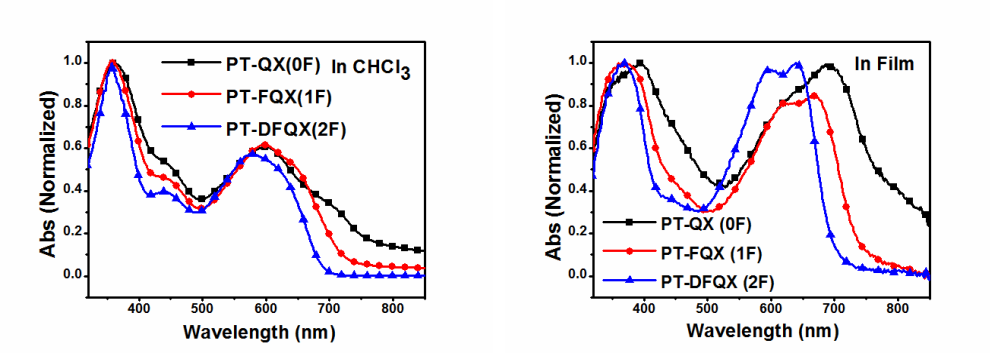

Figure 1. UV−vis absorption spectra of the polymers (a) in chloroform solution and (b) thin films.

Table 2. Optical and Electrochemical Properties of the Polymers

	λ^{max}(nm)						
Polymer	solution	film	λ_{onset}(nm) film	E_g^{opt} (eV)	HOMO/ E_{ox}(eV/V)	LUMO/ E_{red}(eV/V)	E_g^{ec}
PT-QX (0F)	362,600	394,694	772	1.61	-5.10/0.39	-3.53/-1.18	1.57
PT-FQX (1F)	359,597	374,669	738	1.68	-5.18/0.47	-3.54/-1.17	1.64
PT-DFQX (2F)	357,577	369,642	699	1.77	-5.33/0.62	-3.54/-1.17	1.79

2.3 Electrochemical properties

Cyclic voltammetry (CV) was employed to examine the electrochemical properties and determine the highest occupied molecular orbital (HOMO) energy levels and the lowest unoccupied molecular orbital (LUMO) energy levels. The measured cyclic voltammograms are illustrated in Fig 2 and the results are summarized in Table 2. The onset potentials for oxidation (E_{ox}) were 0.39, 0.47 and 0.62 V *vs.* Ag/Ag^+ for PT-QX (0F), PT-FQX (1F) and PT-DFQX (2F), respectively. The related onset potentials for reduction (E_{red}) of them were -1.18,-1.17 and -1.17 V *vs.* Ag/Ag^+, respectively. The energy levels of the HOMO and LUMO of the polymers were calculated according to the equations:[20]

$$HOMO = -e(E_{ox} + 4.71)\ (eV) \quad (1)$$

$$LUMO = -e(E_{red} + 4.71)\ (eV) \quad (2)$$

The HOMO, LUMO, and electrochemical bandgaps (E_g^{ec}) can be calculated from the value of E_{ox} and E_{red} of the copolymers. As shown in Fig S3†, the LUMO energy levels of PT-QX (0F), PT-FQX (1F) and PT-DFQX (2F) are -3.53 eV, -3.54 eV and -3.54 eV, respectively. Thus, one can find that the LUMO energy levels were almost not affected by the introduction of fluorine atoms, and all the three LUMO energy levels are ca. 0.4 eV higher than that of the acceptor $PC_{71}BM$ (-3.91eV), ensuring energetically favorable electron transfer from the polymer donor to the $PC_{71}BM$ acceptor in PSCs. The HOMO energy levels of PT-QX (0F), PT-FQX (1F) and PT-DFQX (2F), are estimated to be -5.10 eV, -5.18 eV and -5.33 eV, respectively. Evidently, the electron-withdrawing nature of the fluorine atom lowers the HOMO energy level of the fluorinated polymer compared with that of the non-fluorinated analog, and the effect is more obvious with the increase of fluorine atom number. As we mentioned before, the low-lying HOMO level is favorable for higher open-circuit voltage (V_{oc}) of the PSCs with the polymers as donor materials because the V_{oc} is usually proportional to the difference between the HOMO level of the donor and the LUMO level of the acceptor. The HOMO level decreases by approximately 0.1 eV

and 0.15 eV as each fluorine atom introduced, which is consistent with the results reported in previous work and theoretical calculations of Muhammet E.Kose *et al*. on other fluorinated copolymers.[21] It is important to emphasize that the incorporation of fluorine does not significantly alter the LUMO levels of the resulting polymer systems, but it does lower the HOMO level of the resulting polymer which is consistent with previous literature.[22] On account of the larger influence on the HOMO energy level in comparison with the LUMO, the electrochemical bandgap (E_g^{ec}) slightly increases upon fluorination. The lower HOMO levels of PT-FQX (1F) and PT-DFQX (2F) can be expected to result in better oxidative stability in ambient conditions and yield a higher open-circuit voltage (V_{oc}) in photovoltaic devices.

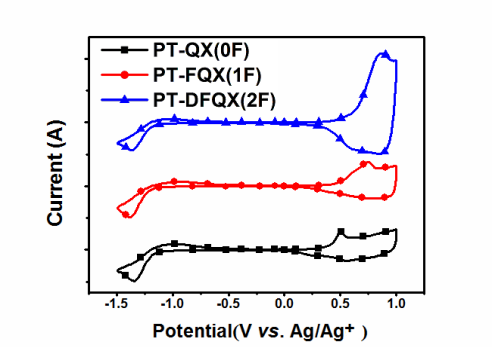

Figure 2. Cyclic voltammograms of the polymer films on a platinum electrode in 0.1 mol/L Bu_4NPF_6 acetonitrile solution at a scan rate of 100 mV/s.

2.4 Photovoltaic properties

The photovoltaic performances of the three polymers were investigated by fabricating BHJ PSCs with the traditional device configuration of ITO/PEDOT:PSS/polymer:$PC_{71}BM$/Ca or ZrAcac/Al. Various methods and conditions were empirically adopted to optimize the PSC devices performance, including the blend ratios of the polymer to $PC_{71}BM$, processing additives, and the modified layer treatment. The measurements of photovoltaic performances were

carried out under an illumination of AM1.5G simulated solar light at 100 mWcm^{-2}. The optimal performance of the devices, such as open-circuit voltage (V_{oc}), short circuit current (J_{sc}), fill factor (FF), and power conversion efficiency (PCE) were summarized in Table 3. Fig 3 shows the representative current density-voltage (J-V) curves of the best performance.

As shown in Table 3, the PCE of devices based on the three polymers present a rising trend along with the number of fluorine atoms. The V_{oc} of the PT-QX (0F), PT-FQX (1F), and PT-DFQX (2F) solar cells are about ~0.6, 0.7, and 0.8 V respectively. Almost ~0.1V increased as each fluorine atom was introduced onto quinoxaline moiety. This phenomenon is consistent with the decrease of 0.08~0.15 eV for the HOMO energy level with every increasing one fluorine atom. Meanwhile the J_{sc} and fill factor（FF）also improved for PT-FQX (1F) and PT-DFQX (2F) compared to PT-QX (0F). The improvement of J_{sc} and FF are mainly owing to the better active layer morphology and appropriate orientation mode as the insertion of fluorine atoms into the quinoxaline moiety (vide infra).

Here, we tried to employ various strategies to further improve the performance of devices. Firstly, we used methanol treatment to modify the interface of active layers,[23] and found that all the devices based on the three polymers showed an increased J_{sc} after methanol treatment (Table.S1†), this might originate from the relatively lower surface resistance caused by the methanol treatment, which is beneficial for charge transport. Then, inspired by recent interfacial modification work[24], we investigated the function of employing commercially available zirconium acetylacetonate (ZrAcac) as a cathode interlayer between the active layer and Al electrode. The well matched energy level of ZrAcac layer and Al is helpful for efficient charge extraction. The results showed that further increase of J_{sc} values, and higher FFs were obtained. Finally, 1,8-Diiodooctane (DIO) was added as processing additive to explore the effect on the performance of the devices. The results indicate that 3% DIO has obvious positive effect on J_{sc} of the devices based on PT-QX (0F) and PT-FQX (1F), but for that of PT-DFQX (2F), the increased J_{sc} is associated with decline of V_{oc} and FF. This is mainly because DIO possess high boiling point (168°C)

and is able to solvate the fullerenes, leading to a comprehensive impact on J_{sc} by providing more optimal morphology for facilitating charge carrier transportation[25]. However the loss of V_{oc} can be attributed to the lowering of charge-separated and charge-transfer-state energies upon additive addition[26]. Simultaneously, we speculate that the addition of DIO decreases the size of fullerene domains and facilitates the formation of a bicontinous interpenetrating donor-acceptor network. Overall, devices with 3% DIO additive exhibited better PCEs than that of the devices without any additive. After treated with all the above optimization method, the PCEs of PT-QX (0F), PT-FQX (1F) and PT-DFQX (2F)-based device are improved from 1.47%, 2.76% and 3.96% to 2.82%, 4.14% and 5.19% respectively, and the corresponding J_{sc} are increased by 57%, 48% and 42% respectively.

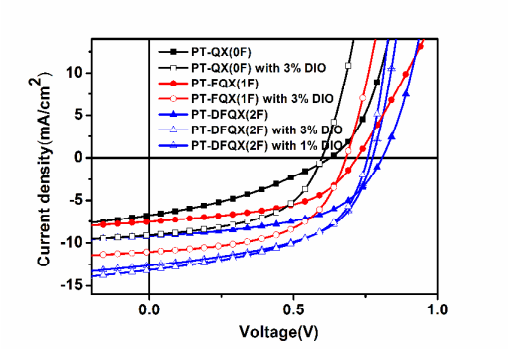

Figure 3. Current density−voltage characteristics of the PSCs based on polymer:$PC_{71}BM$ under illumination of AM1.5G, 100 mW/cm^2.

Table 3. Photovoltaic Performance of the PSCs Based on Polymers/$PC_{71}BM$ under illumination of AM1.5G, 100 mW/cm^2

polymer	Ratio[a]	treatment	V_{oc}(V)	J_{sc}(mA cm^{-2})	*FF*(%)	PCE[b](%)	hole mobilities[c](cm^{2}V^{-1}s^{-1})
PT-QX (0F)	1:1.4	none	0.63	6.76	34.58	1.47	7.27×10^{-5}
PT-QX (0F)	1:1.4	Zracac、3%DIO	0.60	9.10	51.79	2.82	1.07×10^{-4}
PT-FQX (1F)	1:1.3	none	0.72	7.53	50.97	2.76	1.72×10^{-4}

PT-FQX (1F)	1:1.3	Zracac、3%DIO	0.68	11.05	54.92	4.14	5.48×10^{-4}
PT-DFQX (2F)	1:1.2	none	0.81	9.20	53.29	3.96	2.92×10^{-4}
PT-DFQX (2F)	1:1.2	Zracac、1%DIO	0.77	12.62	53.11	5.19	
PT-DFQX (2F)	1:1.2	Zracac、3%DIO	0.76	13.16	51.90	5.17	5.54×10^{-4}

[a]Polymer/$PC_{71}BM$ weight ratio. [b] Optimized data.[c]Measured by using the SCLC method.

The external quantum efficiency (EQE) curves of the devices fabricated under the optimal conditions are shown in Fig 4. All the devices showed broad EQE response range covering the visible region, which is attributed to the intrinsic absorption of both the polymers and $PC_{71}BM$. Among them, the devices based on PT-QX (0F) and PT-FQX (1F) showed similar response range from 300 nm to 800 nm, but the device of PT-DFQX (2F) exhibited significant improvement of EQE in the wavelength range 300-650 nm and a relative narrow absorption. It is important to note that all the EQE spectra showed obvious improvement both in long wavelength region and in short wavelength after DIO addition, which could be ascribed to the change of microstructure of the blend films.

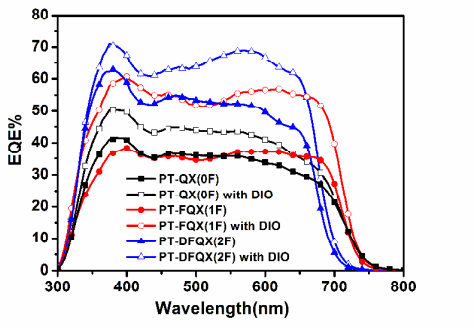

Figure 4. EQE spectra of the PSCs based on polymer/$PC_{71}BM$ blends.

For the convenience of analysis, the absorption spectra of the blend films prepared in the optimal conditions were also measured and are shown in Fig S4†. It is obviously, all the shapes of the EQE spectra for the three devices are in consistent with the absorption spectra of their active layer, and all the J_{sc} of the relative devices were in good agreement with their EQE spectra shown in Fig 4 within an experimental error of 4%. It is worth noting that the blend film comprising PT-DFQX (2F) exhibits higher solid state absorption coefficients, especially in the red part of the spectrum, which explains the reason why the device based on PT-DFQX (2F) exhibited larger J_{sc} than that of the other two.

In consideration of charge-carrier mobilities of the blend films, hole-only devices in a configuration of ITO/PEDOT:PSS/active layer/Au were fabricated and the hole mobilities of the three polymers were measured by using the space-charge-limited current (SCLC) model at low voltage(Fig S5†). The results were summarized in Table 3. Obviously, all of the hole mobilities of the blend films are increased after the Zracac, DIO treatment, which is in well agreement with the J_{sc} and *FF* improvement of the PSCs. However this difference on the mobility among the three polymers is very small, and cannot account for the observed significantly increasing PCEs of the PSCs based on the fluorinated polymers. Thus, it is necessary to characterize the microstructures of the blend films for deeply understanding the effect of F atom on the photovoltaic performance.

2.5 Microstructure

The nano-scale morphology of the active layer plays an important role in the device performance. Proper morphology is not only beneficial for exciton dissociation but also necessary for charge transport to respective electrodes for efficient charge collection[27]. Therefore, tapping mode atomic force microscopy (AFM) measurements were used to investigate the nano-scale morphologies of the polymer/$PC_{71}BM$ blend films. The phase images were taken for the active layer surfaces based on these three

copolymers without and with DIO, and very different morphologies were obtained as shown in Fig 5.

The blend film of PT-QX (0F)/ $PC_{71}BM$ (1 : 1.4, w/w) showed the morphology with average surface roughness (Ra) of 9.103 nm, indicating the clear phase separation and poor compatibility of the blend film. The film of PT-FQX (1F)/$PC_{71}BM$(1 : 1.3,w/w) showed slightly better film morphology with roughness of 2.042 nm, which exhibited moderate homogeneity. The blend film based on PT-DFQX (2F)(1 : 1.2,w/w) showed a morphology with roughness of 1.77 nm and a nanoscale interconnected network structure, indicating that the blend film based on PT-DFQX (2F) provide an adequate combination of polymer solubility and miscibility with $PC_{71}BM$. After these active blend films processed with the additive DIO, all the Ra present a certain degree of decline. It is suggested that the treatment of DIO can promote the films to form a more flat surface and better nano-scale morphology.

As shown in Fig 5, the blend films based on PT-FQX (1F) and PT-DFQX (2F) demonstrated a well-developed fibril structure. Obviously, the appropriate surface appearance associated with the proper roughness is beneficial for exciton diffusion and charge separation, and may effectively assist charge transport prior to recombination. However, blend film based on the PT-QX (0F) showed an inferior morphology with obvious cluster, which may destroy the continuous percolating pathway for hole and electron transport to the corresponding electrodes, consequently increasing the chance of recombination of charge carriers and reducing the J_{sc} accounting for the lower PCE. Moreover, the rough surface will also induce high surface resistance, which is destructive to the performance of solar cells[28]. The results suggest that the introduction of fluorine atoms is beneficial to form an interpenetrated network surrounded by $PC_{71}BM$ phase, and the PT-DFQX (2F)/ $PC_{71}BM$ blend films showed the best combination of bicontinuous nanoscale morphology for efficient charge separation and transport in the polymer/ $PC_{71}BM$ blend film.

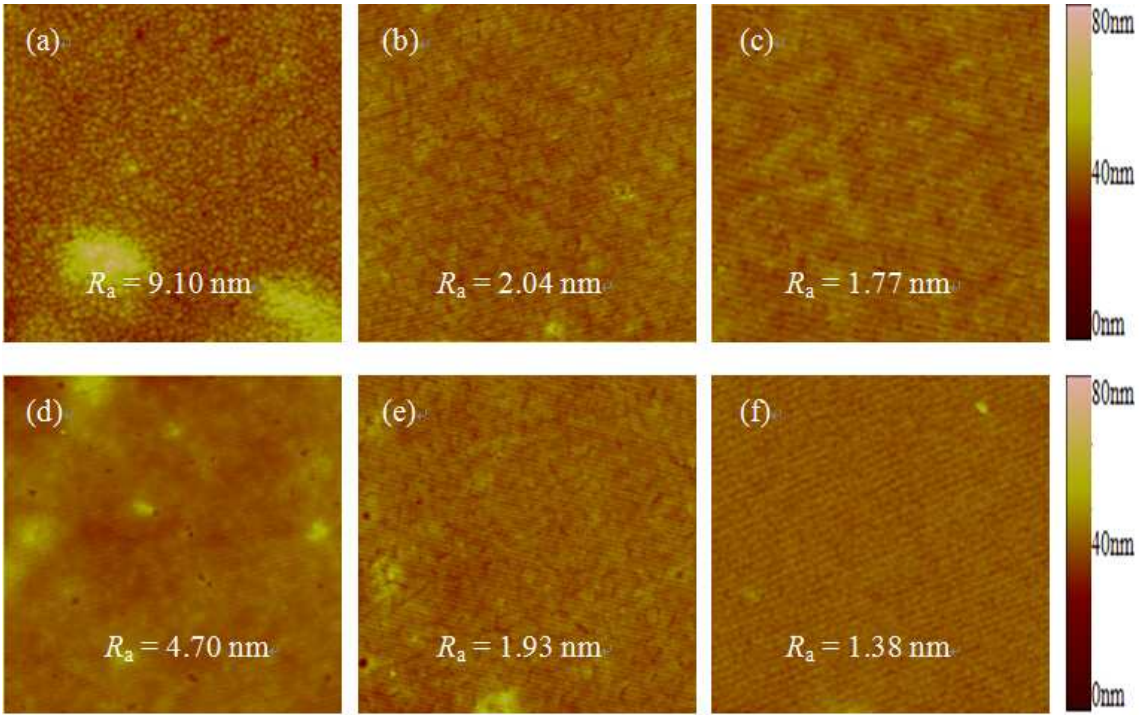

Figure 5. AFM without DIO (top) and with DIO (bottom) images (5 × 5 μm^2) of (a, d) PT-QX (0F) /$PC_{71}BM$ (1:1.4, w/w), (b, e) PT-FQX (1F)/$PC_{71}BM$ (1:1.3, w/w), (c, f) PT-DFQX (2F)/$PC_{71}BM$ (1:1.2, w/w).

In order to deeply study the microstructures of polymers, the preferential orientation of the polymer films were investigated by GIXS. Fig 6 shows the in-plane (IP) and the out-of-plane (OP) GIXS profiles of these three films, and all these polymers films were cast from *o*-DCB (10 mg ml^{-1}). As shown in Fig 6, a relatively stronger IP (100) reflection could be observed for both the PT-FQX (1F) and PT-DFQX (2F) films, while a weak intensity of the (100) reflection occurred in the IP profile of the PT-QX (0F) film. However, the PT-QX (0F) film has a strong OP (100) reflection, which couldn't be observed in both PT-FQX (1F) film and PT-DFQX (2F) film. This indicates that the lamellar packing of PT-FQX (1F) and PT-DFQX (2F) preferentially stacked in the film plane (face-on rich orientation), while the PT-QX (0F) film preferentially stacked out of the film plane (edge-on rich orientation), which suggests that fluorination could make the polymer molecular chain re-orientate, because F

atoms induce crystalline domains in solid state-possibly as a result of favorable C-F⋯H interactions[29]. As well known, this preferential face-on orientation is more beneficial for vertical charge transport than edge-on rich orientation mode, which facilitates charge transport and reduces bimolecular recombination[30], this is in consistent with the enhanced J_{sc} value of the PSCs based on PT-DFQX (2F) and the relative lower J_{sc} value of the PSCs based on PT-QX (0F). In a word, the face-on orientation mode together with the better morphology of the blend film based on PT-DFQX (2F) mentioned above, results in a higher J_{sc} and PCE.

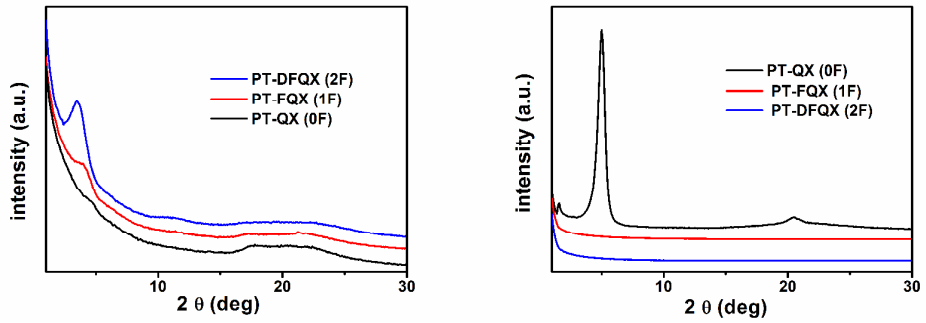

Figure 6. GIXS of polymer thin film in-plane (left), Out-of-plane (right).

3. Conclusion

In order to investigate the effect of fluorine substitution on the optical, electrochemical, photovoltaic properties of the polymers, three D-A conjugated copolymers, named PT-QX (0F), PT-FQX (1F) and PT-DFQX (2F) based on alkylthienyl substituted quinoxaline acceptor unit with different numbers of F substituents and thiophene donor unit were designed and synthesized. The introduction of the fluorine substituents results in gradual decrease in the HOMO levels and slightly blue-shift of the absorption, but almost no influence on the LUMO energy levels of the relative polymers. As a result, the V_{oc} of the resulting PSCs devices increased by approximately 0.1V as each of the F was added. In addition, the J_{sc} was also improved due to the the moderate mobility together with preferential face-on orientation and homogeneous nano-scale morphology caused by the

fluorination. The optimal PSCs devices based on PT-QX (0F), PT-FQX (1F) and PT-DFQX (2F) showed increasing PCE of 2.82%, 4.14% and 5.19%, respectively. Therefore, the introduction of F atoms into the photovoltaic polymers can be considered as an effective strategy to tune the energy levels, active layer morphology and the photovoltaic properties. The deeper research about complicated effects of F atoms on D-A copolymers is worth looking forward.

Experimental section

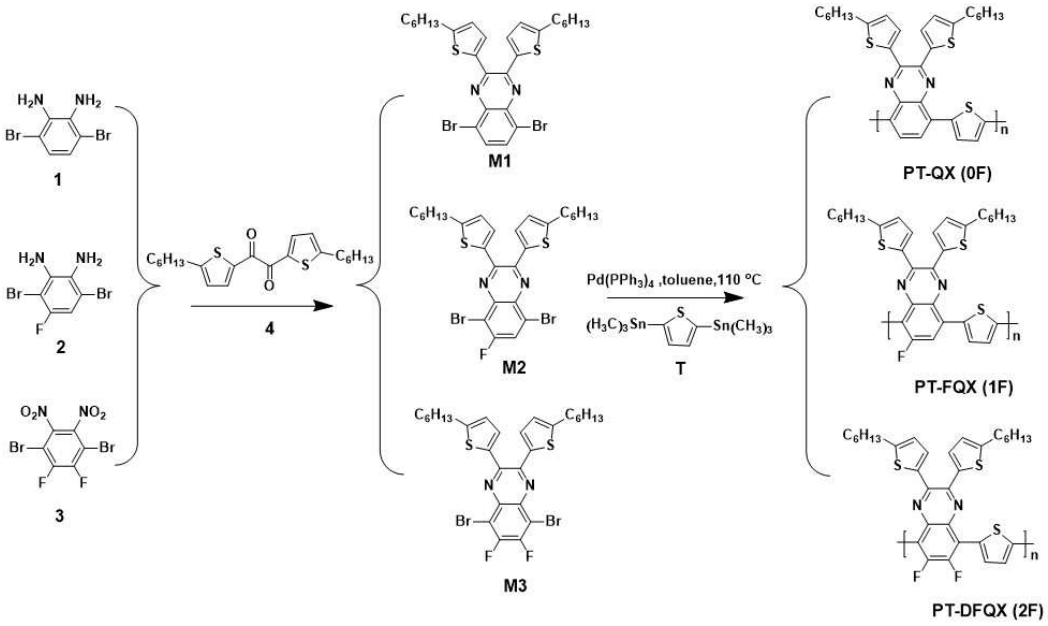

Scheme 2. Synthetic routes of the monomers and the corresponding copolymers.

Materials

Scheme 2 shows the synthetic routes to the copolymers. 1,2-diamino-3,6-dibromobenzene (1)[31(a)], 1,2-diamino-4-fluoro-3,6-dibromobenzene (2)[31 (b)], 1,4-dibromo-2,3-difluoro-5,6-dinitrobenzene (3)[15(a), 31 (c)], 1,2-Bis(5-hexylthiophen-2-yl)ethane-1,2-dione (4) [31(d)] were synthesized according to literature procedures. Tetrahydrofuran (THF) was dried over Na/benzophenone ketyl and freshly distilled prior to use. Other reagents and solvents were of commercial grade and used as received without further purification. All reactions were performed under a nitrogen atmosphere.

5,8-Dibromo-2,3-bis(5-hexylthiophen-2-yl)-quinoxaline(M1)

A mixture of 1,2-dibromo-4-fluoro-1,2-phenylenediamine (1) (0.66 g, 2.5 mmol) and 1,2-bis(5-hexylthiophen-2-yl))ethane-1,2-dione (0.78 g, 2.0 mmol) was dissolved in 30 mL of ethanol and 5 mL of acetic acid. The reaction mixture was heated at 60 °C for 3 h and then cooled down to room temperature. The light yellow precipitate was collected by filtration and washed with ethanol. The crude product was further

purified by column chromatography using 20% dichloromethane and hexane as eluent (yield = 78%, 0.97g). ^{1}H NMR ($CDCl_3$, 600 MHz): δ (ppm): 7.73 (d, 2H),7.47 (d, 2H), 6.79 (d, 2H), 2.95 (d, 4H), 1.59 (d, 4H), 1.30-1.28(br,12H), 0.88 (br,6H)

5,8-Dibromo-6-fluoro-2,3-bis(5-hexylthiophen-2-yl)quinoxaline (M2)

M2 was synthesized by following a similar procedure used for M1, but 1,2-diamino-4-fluoro-3,6-dibromobenzene (2) (0.71g, 2.5 mmol) was used instead of 1,2-diamino-3,6-dibromobenzene (1). Monomer M2 was obtained as a yellow solid (yield = 63%, 0.86g). ^{1}H NMR ($CDCl_3$, 600 MHz): δ (ppm): 7.49-7.44 (br, 3H), 6.81 (d, 2H),2.94 (d, 4H), 1.59 (d, 4H), 1.32-1.28(br,12H), 0.88 (br,6H)

5,8-Dibromo-6,7-difluoro-2,3-bis(5-hexylthiophen-2-yl)quinoxaline (M3)

A mixture of 1,4-dibromo-2,3-difluoro-5,6-dinitrobenzene (1.08 g, 3mmol) and iron powder (2.02 g, 36.0mmol) was added into the acetic acid (100mL), the mixture was briefly heated to 60□, and then the solution was stirred for another 4 h. The residual iron was removed by filtration and 1,2-Bis(5-hexylthiophen-2-yl) ethane-1,2-dione (4) (1.91 g, 3.0mmol) was added to the filtrate, and heated under reflux for 12h. The mixture was poured into water (100mL) and extracted with $CHCl_3$. The extract was then successively washed with water and brine. After drying over anhydrous $MgSO_4$, the solvent was evaporated and subsequently purified by column chromatography on silica gel (eluent: DCM/hexane = 1/7) to afford M3 as a yellow solid (yield = 1.55 g, 79%).^{1}H NMR ($CDCl_3$, 600 MHz): δ (ppm): 7.49 (d, 2H), 6.83 (d, 2H), 2.92 (d, 4H), 1.59 (d, 4H), 1.31-1.29(br,12H), 0.88 (br,6H)

General procedure for polymerization and polymer purification

5,8-Dibromo-2,3-bis(5-hexylthiophen-2-yl)-quinoxaline(M1) (124.0 mg, 0.2 mmol), 5,8-Dibromo-6-fluoro-2,3-bis(5-hexylthiophen-2-yl)quinoxaline (M2) (127.6mg, 0.2 mmol)or 5,8-dibromo-6,7-difluoro-2,3-bis(5-hexylthiophen-2-yl) quinoxaline(M3) (131.4mg, 0. 2 mmol) and 2,5-bis(trimethylstannyl) thiophene (0.2 mmol) were taken

in a 25 mL two-necked flask under an N_2 atmosphere. 8 mL of anhydrous toluene was added and the mixture was degassed for 20 min followed by addition of [$Pd(PPh_3)_4$] (12 mg,0.01 mmol). The mixture was heated at 110 °C for 36h. After cooling to room temperature, it was poured into vigorously stirred methanol (300 mL) together with 30 mL of 30% aqueous NH_4OH solution and the resulting precipitate was filtered and washed with methanol (2 × 200 mL). The polymer was purified by Soxhlet extraction using methanol (18 h), acetone (18 h) and hexane (18 h), and finally extracted with chloroform. The chloroform solution was then concentrated by evaporation and re-precipitated in methanol. The resulting solid was collected and dried overnight under vacuum. The polymers were characterized by ^{1}H NMR, GPC, and elemental analysis.

Poly-thiophene-alt-2,3-bis(5-hexylthiophen-2-yl)-quinoxaline (PT-QX (0F))

Isolated yield = 47%. GPC analysis Mn =13.1kDa, Mw = 20.7 kDa, and PDI = 1.58 (against PS standard). ^{1}H NMR ($CDCl_3$, 600 MHz): δ (ppm): 7.89-7.69 (br, 4H), 7.49-6.82 (br, 6H), 3.18 (br, 2H), 1.59–0.88 (br, 24H); anal. calcd for $C_{32}H_{36}N_2S_3$: C, 70.54; H, 6.66; N, 5.14; S, 17.66; found: C, 70.95; H, 6.20; N, 5.36; S, 17.49.

Poly-thiophene-alt-6-fluoro-2,3-bis(5-hexylthiophen-2-yl)quinoxaline (PT-FQX (1F))

Isolated yield = 67%. GPC analysis Mn = 14.3 kDa, Mw = 24.7 kDa, and PDI = 1.73 (against PS standard). ^{1}H NMR ($CDCl_3$, 600 MHz): δ (ppm): 7.73-6.83 (br, 9H), 2.94

(br, 2H), 1.59–0.88 (br, 24H); anal. calcd for $C_{32}H_{35}FN_2S_3$: C, 68.29; H, 6.27; N, 4.68; S, 17.09; found: C, 67.95; H, 6.14; N, 5.17; S, 17.23.

Poly-thiophene-alt- 6,7-difluoro-2,3-bis(5-hexylthiophen-2-yl) quinoxaline (PT-DFQX (2F))

Isolated yield = 87%. GPC analysis Mn = 16.6 kDa, Mw = 28.6 kDa, and PDI = 1.73 (against PS standard). ^{1}H NMR ($CDCl_3$, 600 MHz): δ (ppm): 7.69-6.81 (br, 8H), 2.77 (br, 2H), 1.59–0.88 (br, 24H); anal. calcd for $C_{32}H_{34}F_2N_2S_3$: C, 66.17; H, 5.90; N, 4.82; S, 16.56; found: C, 67.34; H, 6.05; N, 4.17; S, 16.23.

Characterization

The molecular weight of the polymer was measured using gel permeation chromatography (GPC) with polystyrenes as reference standard and TCB as an eluent. All new compounds were characterized by nuclear magnetic resonance spectra (NMR). The NMRs were recorded on a Bruker AV 600 MHz or 400 MHz spectrometer in Trichlorobenzene (TCB) at 150°C using tetramethylsilane (TMS; δ = 0 ppm) as an internal standard. Elemental analyses were performed on a Flash EA 1112 elemental analyzer. Thermal gravimetric analysis (TGA) measurements were carried out on PerkinElmer TGA 4000 under a nitrogen atmosphere at a heating rate of 10 °C/min. Differential scanning calorimetry (DSC) measurements were conducted using a Mettler Toledo DSC 1 in a temperature range from 25-250 °C under nitrogen at a heating rate of 5 °C/min. UV–vis–NIR absorption spectra were measured on Shimadzu spectrometer model UV-3150. The electrochemical cyclic voltammetry

was recorded on a Zahner Ennium Electrochemical Workstation with a glass carbon disk (coated with the polymer film), a Pt wire, and Ag/Ag^+ electrode as working electrode, counter electrode and reference electrode respectively in a 0.1 mol/L tetrabutylammonium hexafluorophosphate (Bu_4NPF_6) acetonitrile solution. X-ray diffraction (XRD) measurements were carried out in a reflection mode, using a D/MAX-TTR III Rigaku X-ray diffraction system. Atomic force microscopy (AFM) measurements were carried out on a Digital Instruments Nanoscope V instrument, and operated in a tapping mode.

Fabrication and characterization of photovoltaic devices

The PSCs were fabricated with a configuration of ITO/PEDOT:PSS (40 nm)/active layer/cathode. A thin layer of PEDOT:PSS (poly(3,4-ethylenedioxythiophene):poly(styrenesulfonate)) was deposited through spin-coating on pre-cleaned ITO-coated glass with a PEDOT:PSS aqueous solution (Baytron PVP AI 4083 from H.C. Starck) at 3000 rpm and dried subsequently at 150 °C for 15 min in air, then the devices was transferred to a nitrogen glove box, where the active blend layer of the polymer and fullerene derivative was spin-coated onto the PEDOT:PSS layer. For conjugated polymer: $PC_{71}BM$ PSCs, the active layer was formed by spin coating with ortho-dichlorobenzene (o-DCB) solution containing 8～10 mg ml^{-1} polymer. The ZrAcac cathode interlayer was simply prepared by spin-coating an ethanol solution (1 mg ml^{-1}) on the photoactive layer at 3000 rpm for 30s at room temperature, no thermal annealing or any other post-treatment was performed. Finally, the top electrode was deposited in a vacuum onto the active layer. The active area of the device was 4 mm^2. The thickness of the photosensitive layer was ca. 60-120nm, measured using an Ambios Tech XP-2 profilometer. The current density-voltage (J-V) characteristics were measured using a computer-controlled

Keithley 236 Source-Measure Unit. Axenon lamp (150W) coupled with AM 1.5 solar spectrum filter was used as the light source, and the optical power at the sample was 100 mW cm^{-2}. External quantum efficiency (EQE) spectrum was easured by a Stanford Research Systems model SR830 DSP lock-in amplifier coupled with WDG3 monochromator and a 150 W xenon lamp.

The divices for the hole mobility measurement were fabricated using the architectures: ITO/PEDOT:PSS/polymer:$PC_{71}BM$/Au. The diveces for the hole mobility were calculated by fitting the current density-voltage (J-V) curves using the Mott-Gurney relationship (space-charge limited current, SCLC). The SCLC can be approximated by the eqn:

$$J \cong \frac{9}{8}\varepsilon_r\varepsilon_0\mu_0 \exp\left(0.891\gamma\sqrt{\frac{V}{L}}\right)\frac{V^2}{L^3}$$

Here J is the current density, ε_r is the dielectric constant of the polymer, ε_0 is the free-space permittivity (8.85×10^{-12} F/m), μ_0 is the charge mobility at zero field, γ is a constant, L is the thickness of the blended film layer, $V=V_{appl}-V_{bi}$, V_{appl} is the applied potential, and V_{bi} is the built-in potential which results from the difference in the work function of the anode and the cathode (in hole device architecture, $V_{bi} = 0.2$ V).

Corresponding Author

* E-mail: wanghaiqiao@mail.buct.edu.cn (H. Wang); liyf@iccas.ac.cn (Y. Li); lixy@mail.buct.edu.cn (X. Li)

ACKNOWLEDGMENT

This work was supported by Beijing Natural Science Foundation (2122047) and Specialized Research Fund for the Doctoral Program of Higher Education (20130010110006). The GIXS data was obtained at 1W1A, Beijing Synchrotron

Radiation Facility. The authors gratefully acknowledge the assistance of scientists of the Diffuse X-ray Scattering Station during the experiments.

REFERENCES

(1) (a) Jhong-Sian Wu, Sheng-Wen Cheng, Yen-Ju Cheng and Chain-Shu Hsu, *Chem. Soc. Rev.*, 2014, **10**, 29. (b) Gang Li, Rui Zhu and Yang Yang, *Nature. Photonics*, 2012, **6**, 153. (c) Li X, Choy, W. C. H, Huo L, Xie F., Sha, W. E. I, Ding B, Guo X, Li Y, Hou J, You J and Yang Y, *Adv. Mater.,* 2012, **24**, 3046–3052.

(2) (a) Liao S-H, Jhuo H-J, Yeh P-N, Cheng Y-S, Li Y-L, Lee Y-H, et al., *Sci. Rep.*, 2014, **4**. (b) Liu Y, Zhao J, Li Z, Mu C, Ma W, Hu H, et al., *Nat. Commun*, 2014, **5**.

(3) (a) Zhou H, Yang L, Stoneking S, You W, *ACS. Appl. Mater. Interfaces.,* 2010, **2**, 1377–1383. (b) Price S.C, Stuart A.C, Yang L, Zhou H, You W, *J. Am. Chem. Soc.,* 2011, **133**, 4625–4631. (c) H. L. Zhong, Z. Li, F. Deledalle, E. C. Fregoso, M. Shahid, Z. P. Fei, C. B. Nielsen, N. Y. Gross, S. Rossbauer, T. D. Anthopoulos, J. R. Durrant, and M. Heeney, *J. Am. Chem. Soc.*, 2013, **135**, 2040. (d) Chaohua Cui, Wai-Yeung Wong and Yongfang Li, *Energy Environ.Sci*. 2014, **7**, 2276-2284. (e) Zhicai He, Chengmei Zhong, Xun Huang, Wai-Yeung Wong, Hongbin Wu, Liwei Chen, Shijian Su and Yong Cao, *Adv.Mater.,* 2011, **23**, 4636-4643. (f) Wai-Yeung Wong, Xing-Zhu Wang, Ze He, Aleksandra B. Djurisic, Cho-Tung Yip, Kai-Yin Cheung, Hai Wang, Chris S.K.Mak and Wai-Kin Chan, Nat.Mater., 2007, **6**, 521.

(4) (a) Thompson B. C., Fréchet, J. M. J., *Angew. Chem., Int. Ed.* 2008, **47**, 58–77. (b) Chen J., Cao Y., *Acc. Chem. Res.* 2009, **42**, 1709–1718. (b) J. H. Kim, C. E. Song, B. S. Kim, I. N. Kang and D. H. Hwang, *Chem. Mater.*, 2014, **26**, 1234. (c) Zhou H, Yang L, You W, *Macromolecules* 2012, **45**, 607–632. (d) Y. F. Li, *Acc. Chem. Res.*,

2012, **45**, 723. (e) Wai-Yeung Wong and Cheuk-Lam Ho, *Acc. Chem. Res*., 2010, **43**, 1246.

(5) (a) Long Ye, Shaoqing Zhang, Wenchao Zhao, Huifeng Yao and Jianhui Hou*, Chem. Mater.,* 2014, **26**, 3603. (b) Kui Feng, Xiaopeng Xu, Zuojia Li, Ying Li, Ting Yu and Qiang Peng, *Chem. Comm.*, 2015, **10**, 1039. (c) Sungmin Park, Dongkyun Seo, Tae In Ryu, Gukil Ahn, Kyung Won Kwak, Hyunjung Kim, et al., *Macromolecules,* 2014, **10**, 1021. (d) Tianshi Qin, Wojciech Zajaczkowski, Wojciech Psisula, Martin Baumgarten, Ming Chen, Mei Gao, Gerry Wilson, Christopher D. Easton, et al*., J. Am. Chem. Soc.,* 2014*,* **136***,* 6049−6055. (e) Lai Fan Lai, John A.Love, Alexander Sharenko, Jessica E.Coughlin, Vinay Gupta, Sergei Tretiak, Thuc-Quyen Nguyen, Wai-Yeung Wong, and Guillermo C.Bazan., *J. Am. Chem. Soc.* 2014*,* **136***,* 5591−5594.

(6) (a) Hsieh-Chih Chen, Ying-Hsiao Chen, Chi-Chang Liu, Yun-Chen Chien, Shang-Wei Chou and Pi-Tai Chou, *Chem. Mater.,* 2012, **24**, 4766. (b) Xiaowei Jia, Weiyi Zhang, Xuefeng Lu, Zhong-Sheng Wang and Gang Zhou, *J. Mater. Chem. A.*, 2014, **2**, 19515. (c) Thomas S.van Der Poll, John A.Love Thuc-Quyen Nguyen and Guillermo C.Bazan., *Adv.Mater.,* 2012, **24**, 3646. (d) Yunzhang Lu, Zhengguo Xiao, Yongbo Yuan, Haimei Wu, Zhongwei An, Yanbing Hou, Chao Gao and Jinsong Huang*, J. Mater. Chem. C.,* 2013*,* **1***,* 630−637.

(7) (a) Jae Woong Jung, Jea Woong Jo, Chu-Chen Chueh, Feng Liu, Won Ho Jo, Thomas P.Russell and Alex K-Y.Jen*., Adv. Mater.,* 2015, **10**, 1002. (b) Jae Woong

Jung, Seunghwan Bae, Feng Liu, Thomas P.Russell and Won Ho Jo, *Adv. Funct. Mater.,* 2015, **25**, 120.

(8) (a) Weichao Chen, Zhengkun Du, Liangliang Han, Manjun Xiao, Wenfei Shen, Ting Wang, Yuanhang Zhou and Renqiang Yang, *J. Mater. Chem. A.*, 2015, **3**, 3130. (b) Xiaowei Jia, Weiyi Zhang, Xuefeng Lu, Zhong-Sheng Wang and Gang Zhou, *J. Mater. Chem. A.*, 2014, **2**, 19515. (c) Thomas S.Van Der Poll, John A.Love Thuc-Quyen Nguyen and Guillermo C.Bazan, *Adv. Mater.,* 2012, **24**, 3646. (d) Yunzhang Lu, Zhengguo Xiao, Yongbo Yuan, Haimei Wu, Zhongwei An, Yanbing Hou, Chao Gao and Jinsong Huang, *J. Mater. Chem. C.,* 2013*,* **1***,* 630−637.

(9) (a) Hoaxing Zhou, Liqiang Yang, Andrew C.Stuart, Samuel C. Price, Shubin Liu and Wei You, *Angew.Chem.,* 2011, **123**, 3051. (b) Samuel C.Price, Andrew C.Stuart, Liqiang Yang, Huaxing Zhou and Wei You, *J. Am. Chem. Soc.*, 2011, **133**, 4625. (c) Steve Albrecht, Silvia Janietz, Wolfram Schindler, Johannes Frisch, Jona Kurpiers, Juliane Kniepert and Sahika Inal, et al., *J. Am. Chem. Soc.,* 2012, **134**, 14932.

(10) Yun-Xiang Xu, Chu-Chen Chueh, Hin-Lap Yip, Fei-Zhi Ding, Yong-Xi Li, Xiaosong Li, Wen-Chang Chen and Alex K.-Y.Jen, *Adv. Mater.,* 2012, **24**, 6356.

(11) Yong Zhang, Shang-Chieh Chien, Kung-Shih Chen, Hin-Lap Yip, Ying Sun, Joshua A.Davies, Fang-Chung Chen and Alex K.-Y. Jen, *Chem.Commun.,* 2011, **47**, 11026-11028.

(12) (a) Akila Lyer, Josiah Bjorgaard, Trent Anderson and Muhammet E.Kose, *Macromolecules*, 2012, **45**, 6380-6389. (b) Samuel C.Price, Andrew C.Stuart, Liqiang

Yang, Huaxing Zhou and Wei You, *J. Am. Chem. Soc.*, 2011, **133**, 4625. (c) Yong Zhang, Jingyu Zou, Chu-Chen Cheuh, Hin-Lap Yip and Alex K.-Y. Jen, *Macromolecules*, 2012, **45**, 5427-5435.

(13) (a) Bob C.Schroeder, Zhenggang Huang, Raja Shahid Ashraf, Jeremy Smith, Rasquale D'Angelo, Scott E.Watkins, Thomas D.Anthopoulos, James R. Durrant and Lain McCulloch, *Adv. Funct. Mater.*, 2012, **22**, 1663-1670. (b) Zhao Li, Jianping Lu, Shing-Chi Tse, Jiayun Zhou, Xiaomei Du, Ye Tao and JianFu Ding, *J. Mater. Chem.,* 2011, **21**, 3226-3233. (c) Yun-Xiang Xu, Chu-Chen Chueh, Hin-Lap Yip, Fei-Zhi Ding, Yong-Xi Li, Xiaosong Li, Wen-Chang Chen and Alex K.-Y.Jen, *Adv. Mater.,* 2012, **24**, 6356.

(14) (a)Ergang Wang, Jonas Bergqvist, Koen Vandewal, Zaifei Ma, Lintao Hou, Angelica Lundin, Scott Himmelberger, Alberto Salleo, Christian Muller, Olle Ingands, Fengling Zhang and Mats R.Andersson, *Adv. Energy. Mater.*, 2013, **3**, 806-814. (b) Ji-Hoon Kim, Chang Eun Song, Hee Un Kim, Andrew C.Grimsdale, Sang-Jin Moon, Won Suk Shin, Si Kyung Choi and Do-Hoon Hwang, *Chem. Mater.,* 2013, **25**, 2722-2732. (c) Dongfeng Dang, Weichao Chen, Scott Himmelberger, Qiang Tao, Angelica Lundin, Renqiang Yang, Weiguo Zhu, Alberto Salleo, Christian Muller and Ergang Wang, *Adv. Energy. Mater.,* 2014, **4**, 1400680.

(15) (a)Meng Wang, Di Ma, Keli Shi, Shaowei Shi, Song Chen, Changjiang Huang, Zi Qiao, Zhi-Guo Zhang, Yongfang Li, Xiaoyu Li and Haiqiao Wang, *J. Mater. Chem. A.*, 2015, **3**, 2802-2814. (b) Lidia Marin, Laurence Lutsen, Dirk Vanderzande and

Wouter Maes, *Org. Biomol. Chem.,* 2013, **11**, 5866-5876. (c) R. M. Duan, L. Ye, X. Guo, Y. Huang, P. Wang, S. Q. Zhang, J. P. Zhang, L. J. Huo and J. H. Hou, *Macromolecules*, 2012, **45**, 3032. (d) Hsieh-Chih Chen, Ying-Hsiao Chen, Chung-Hao Liu, Yen-Hao Hsu, Yun-Chen Chien, Wei-Ti Chuang, Chih-Yang Cheng, Chien-Liang Liu, Shang-Wei Chou, Shih-Huang Tung and Pi-Tai Chou, *Polym. Chem.*, 2013, **4**, 3411-3418.

(16) Samuel C.Price, Andrew C.Stuart, Liqiang Yang, Huaxing Zhou and Wei You, *J. Am. Chem. Soc.*, 2011, **133**, 4625-4631.

(17) Xiaochen Wang, Pei Jiang, Yu Chen, Hao Luo, Zhiguo Zhang, Haiqiao Wang, Xiaoyu Li, Gui Yu and Yongfang Li, *Macromolecules,* 2013, **46**, 4805−4812.

(18) D. Dang, W. Chen, S. Himmelberger, Q. Tao, A. Lundin, R. Yang, W. Zhu, A. Salleo, C. Muller and E. Wang, *Adv. Energy. Mater.,* 2014, DOI:10.1002/aenm.201400680.

(19) H.J.Son, W.Wang, T.Xu, Y.Y.Liang, Y.E.Wu, G.Li and L.P.Yu, *J. Am. Chem. Soc.*, 2011, **133**, 1885-1894.

(20) (a) Sun Q. J, Wang H. Q, Yang C. H., Li Y. F, *J. Mater. Chem.*, 2003, **13**, 800-806. (b) Hou J. H, Tan Z. A, Yan Y, He Y. J, Yang, C. H, Li Y. F, *J. Am. Chem. Soc.,* 2006, **128**, 4911-4916. (c) Wang X, Sun Y, Chen S, Guo X, Zhang M, Li X, Li Y and Wang H, *Macromolecules,* 2012, **45**, 1208−1216.

(21) (a)Pieter Verstappen, Jurgen Kesters, Wouter Vanormelingen, Gael H.L.Heintges, Jeroen Drijkoningen, Tim Vangerven, Lidia Marin, Simplice Koudjina, Benoit

Champagne, Jean Manca, Laurence Lutsen, Dirk Vanderzande and Wouter Maes, *J. Mater. Chem. A.*, 2015, **3**, 2960-2970. (b)A.Iyer, J.Bjorgaard, T. Anderson and M.E.Kose, *Macromolecules*, 2012, **45**, 6380-6389.

(22) (a) T.Umeyama, Y.Watanabe, E.Douvogian Ni and H.Imahori, *J. Phys. Chem. C.*, 2013, **117**, 21148-21157. (b) H.Zhou, L.Yang, A.C.Stuart, S.Cprice, S.Liu and W.You, *Angew. Chem., Int.Ed*, 2011, **50**, 2995-2998.

(23) (a) Wang. Y, Liu. Y, Chen. S, Peng. R and Ge. Z, *Chem. Mater.*, 2013, **25**, 3196. (b) Zhou. H, Zhang. Y, Seifter. J, Collins. S. D, Luo. C, Bazan. G. C, Nguyen. T. Q, Heeger. A. J, *Adv. Mater.*, 2013, **25**, 1646. (c) P. Shen, H. J. Bin, L. Xiao and Y. F. Li, *Macromolecules*, **2013**, *46*, 9575.

(24) (a) Jae Kwan Lee, Wan Li Ma, Christoph J. Brabec, Jonathan Yuen, Ji Sun Moon, Jin Young Kim, Kwanghee Lee, Guillermo C.Bazan and Alan J.Heeger, *J. Am. Chem. Soc.*, 2008, **130**, 3619-3623. (b)Joseph W. Rumer, Raja S. Ashraf, Nancy D.Eisenmenger, Zhenggang Huang, Iain Meager, Christian B.Nielsen, Bob C.Schroeder, Michael L.Chabinyc and Iain McCulloch, *Adv. Energy. Mater.*, 2015, **5**, 1401426. (c) Sylvia J. Lou, Jodi M.Szarko, Tao Xu, Luping Yu, Tobin J.Marks and Lin X.Chen, *J. Am. Chem. Soc.*, 2011, **133**, 20661-20663.

(25) (a) Peet, J.Kim, J.Y, Coates, N.E., Ma, W.L., Moses, D.Heeger, A.J.Bazan, G.C., *Nat. Mater.*, 2007, **6**, 497-500. (b)Lee, J.K.Ma, W.L.Brabec, C.J.Yuen, J.Moon, J.S.Kim, J.Y.Lee, K.Bazan, G.C.Heeger, A., *J. Am. Chem. Soc.*, 2008, **130**, 3619-3623.

(26) Nuzzo, D.Di.Aguirre, A.Shahid, M.Gevaerts, V.S.Meskers, S.C.J.Janssen, et al., *Adv. Mater.*, 2010, **22**, 4321-4324.

(27) (a) W.L.Leong, S.R.Cowan and A.J.Heeger, *Adv. Energy. Mater.*, 2011, **1**, 517-522. (b)A.Baumann, T.J.Savenije, D.H.K.Murthy, M.Heeney, V.Dyakonov and C.Deibel, *Adv. Funct. Mater.*, 2011, **21**, 1687-1692. (c) H.Zang, Y.Liang, L.Yu and B.Hu, *Adv. Energy. Mater.*, 2011, **1**, 923-929.

(28) Jea Woong Jo, Seunghwan Bae, Feng Liu, Thomas P.Russell and Won Ho Jo, *Adv.Funct.Mater.*, 2015, **25**, 120-125.

(29) Weichao Chen, Zhengkun Du, Liangliang Han, Manjun Xiao, Wenfei Shen, Ting Wang, Yuanhang Zhou and Renqiang Yang, *J. Mater. Chem. A.*, 2015, **3**, 3130.

(30) (a) Itaru Osaka, Takeshi Kakara, Noriko Takemura, Tomoyuki Koganezawa and Kazuo Takimiya, *J. Am. chem. Soc.*, 2013, **135**, 8834–8837. (b) Itaru Osaka, Masafumi Shimawaki, Hiroki Mori, Iori Doi, Eigo Miyazaki, Tomoyuki Koganezawa and Kazuo Takimiya, *J. Am.chem.Soc*, 2012, **134**, 3498–3507.

(31) (a) Dinesh G. P, Fude F, Yu. O, Khalil A. A, So H, Kirk S. S and John R. R, J. *Am. Chem. Soc.*, 2012, **134**, 2599–2612. (b) Gitish K. D, Taehyo K, Hyo. S. C, Jung. H. L, Dong S. K, Jin. Y. K and Chang. D. Y, *Polym. Chem.*, 2014, **5**, 2540-2547. (c) Meng Wang, Shaowei Shi, Di Ma, Keli Shi, Chen Gao, Liwei Wang, Gui Yu, Yongfang Li, Xiaoyu Li and Haiqiao Wan, *Chem. Asian J*, **2014**, 9, 2961–2969. (d) Li Shuang, He Zhicai, Yu Jian, et al., *Polym. Sci. A Polym. Chem.*, 2012, **50**, 2819-2828.

For “Table of Content” only

Effect of Fluorine Substitution on the Photovoltaic Performance of Poly(thiophene-quinoxaline) Copolymers

Zi Qiao, Meng Wang, Mingzhi Zhao, Zhiguo Zhang, Yongfang Li, Xiaoyu Li, Haiqiao Wang